The Egyptian Journal of Radiology and Nuclear Medicine 47 (2016) 1303–1311

Contents lists available at ScienceDirect

The Egyptian Journal of Radiology and Nuclear Medicine

journal homepage: www.sciencedirect.com/locate/ejrnm

Original Article

The coronary arterial anatomy of the 17-segment model using 3-Tesla cardiac magnetic resonance imaging

Mohamed Talaat [a], Ahmed Kharabish [a,b,*], Mohamed D. Homos [a], Mohamed Fouad [a], Doaa Mohamed Nabil [a]

[a] Department of Radiology, Cairo University Hospitals, 11256 Cairo, Egypt
[b] Department of Radiology, Aswan Heart Center, Aswan, Egypt

ARTICLE INFO

Article history:
Received 2 April 2016
Accepted 23 June 2016
Available online 22 July 2016

Keywords:
Cardiovascular magnetic resonance
3T
Myocardial scarring
17-segment model

ABSTRACT

Aim: To analyze the correspondence of the 17 left ventricular myocardial segments with each coronary artery by using late gadolinium contrast enhanced cardiovascular magnetic resonance (CMR) imaging.
Material and methods: A total number of 58 patients with known or suspected ischemic heart disease were enrolled in this study. Those patients were scheduled for CMR and conventional coronary angiography. The correspondence between the coronary artery distribution and the supplied myocardium was assessed according to the 17-segment model.
Results: The segments 1, 2, 3, 7, 8, 13, 14 and 17 were totally specific for LAD, segments 6 and 12 were totally specific for LCX, and segment 10 was specific for RCA. There was overlap between LAD and RCA for segments 9 and 15. There was overlap between LCX and RCA for segments 4, 5 and 11. The segment 16 was shared by the all territories (LAD, LCX and RCA) with slight LCX predominance.
Conclusions: Our study concluded that the LAD territory on CMR bases is larger than the American Heart Association (AHA) proposed 17-segment model.

1. Introduction

Coronary artery disease (CAD) is a leading cause of death worldwide [1]. It is important to study coronary arterial tree and correlate its anatomy with the different imaging tools in order to plan the revascularization prior to invasive angiography. Earlier studies were performed using different imaging modalities such as nuclear cardiology, echocardiography and cardiac computed tomography to define cardiac planes and segmentations in 2-dimensional (2D) or tomographic imaging.

The left ventricular segmentations and assignment of these segments to coronary arterial territories are still not sharply defined and confusing. First, the great variation of the different coronary artery anatomies results in overlap in the supply of the ventricular segments and this could be partially explaining this dilemma. Second, the limited studies and researches concerned with the assignment of these segments to coronary arterial territories [2]. Third, the different imaging modalities used in prior studies make difficult comparison. Fourth, most of the prior researches is based on myocardial perfusion SPECT study. The SPECT is the most widely used technique to assess CAD but it has several limitations as attenuation artifacts, its low spatial

Peer review under responsibility of The Egyptian Society of Radiology and Nuclear Medicine.
* Corresponding author at: Cairo University Hospitals, 11256 Cairo, Egypt.
E-mail address: Ahmedkharabish@hotmail.com (A. Kharabish).

http://dx.doi.org/10.1016/j.ejrnm.2016.06.021
0378-603X/

resolution and limited ability to detect sub-endocardial defects [2].

In the last decade, cardiovascular magnetic resonance (CMR) has evolved into a new technique for the noninvasive detection of CAD. The advances in MR machines, cardiac techniques and powerful gradients, shorten the cardiac MR exam and expand its clinical uses [3]. Regarding the CAD, the cardiovascular magnetic resonance (CMR) can assess the ventricular function, motion abnormality, localization of ischemic viable and non-viable segments in single examination. In addition, it clearly diagnoses the associated complications of myocardial infarction as cardiac aneurysm or valvular disease [4]. The CMR has great advantages particularly the high degree of spatial and temporal resolution (which is sufficient to detect micro-infarct and differentiate between subendocardial and subepicardial infarcts) without the need of radioactive tracer administration [2–5].

Therefore cardiac segmentations and their assignment to coronary arterial territories should be standardized and interpreted using CMR.

Many previous studies were performed to assess the left ventricular segmentations, forming many different segmentation models, ranging between 9 and 64 segments [6–18]. The 17-myocardial segment model for mapping coronary artery territories was recommended by the American Heart Association (AHA) and currently widely used in clinical practice [19]. On the contrary, other studies have been carried out confirmed the inaccuracy of this mapping between the 17 segments and the coronary arteries and these studies suppose different mappings [18].

The goal of the present study was to use and analyze the correspondence of the 17 myocardial segment model of the left ventricle with each coronary artery by using contrast enhanced CMR imaging.

2. Patients and methods

A total number of 58 patients with known or suspected ischemic heart disease were enrolled in this study starting from October 2012 to February 2015. Those patients were referred to our institute from the different ICU and cardiology departments. All patients signed consent for participation in the study, and then they were scheduled for CMR and conventional coronary angiography within maximum 3 weeks in-between.

2.1. Inclusion criteria

(1) Attack of chest pain for at least half an hour with ECG or laboratory finding suspicion of myocardial infarction.
(2) Detection of myocardial fixed defect (myocardial scarring) by Sestamibi study.

2.2. Exclusion criteria

(1) Contraindications for MR imaging; claustrophobia, patients with pacemaker or metal implants.
(2) Contraindication for contrast material, including known allergy and renal insufficiency (serum creatinine more than 1.4 mg/dl).
(3) Hemodynamic instability.
(4) Atrial fibrillation.
(5) Subjects with previous coronary bypass surgery.

2.3. Patient preparation and setup

No special instructions are required prior to the examination. Medications are not to be discontinued.

First, a short medical history was taken. Patients were then screened for contraindication to MR imaging. All undergarments containing nylon or metal were removed.

Before the examination: All steps of the study were explained in detail for each patient, such as breath-holding (i.e., Valsalva maneuver) for relatively long time. The heart rate and rhythm were evaluated.

2.4. CMR

The patients were examined using 3.0-T Philips Achieva scanner (Philips Achieva, Netherland) in supine position. Dedicated cardiac phased-array receiver coil was used. The study begins with scout views in orthogonal directions and set of different cardiac planes (short and long axis views). Bolus of 0.2 mmol/kg gadopentetate dimeglumine (Magnevist) was injected intravenously, followed by 5 cm saline. Cine loop images were taken during breathholds using b-FFE (Balanced Fast Field Echo) in short axis slices covering the heart from the mitral annulus to the LV apex and in one long axis view (two or four chamber views) with the following parameters: TR/TE: 4.4/2.5, FOV: $300 \times 300\ mm^2$, Phases: 25, NSA: 1, Matrix: 128×128, Slice thickness: 8 mm, Slice number: 8-11.

About ten minutes following the injected contrast, delayed contrast enhanced images were acquired in short axis and at least one of the long axes using inversion-recovery (IR) segmented gradient-echo sequence. Look-locker sequence was performed before IR sequence to adjust the optimum inversion time for nulling the normal myocardium (ranging between 250 and 330 ms). The IR sequence performed with the following parameters: TR/TE: 40/4, Field of view: 360–400 mm, matrix size: 256×256, NSA: 2, Slice thickness: 8 mm and Slice number: 7-11.

2.5. Coronary angiography

All patients were scheduled for diagnostic coronary angiography using a trans-femoral approach to selectively inject the left and right coronary systems sequentially. All studies were interpreted by expert angiographer who is masked to the results of CMR. Arterial catheterization and selective coronary angiography were performed within 3 weeks after the cardiac MR study. Different projections are used according to the standard techniques with at least four views of the left and two views of the right coronary artery systems were analyzed.

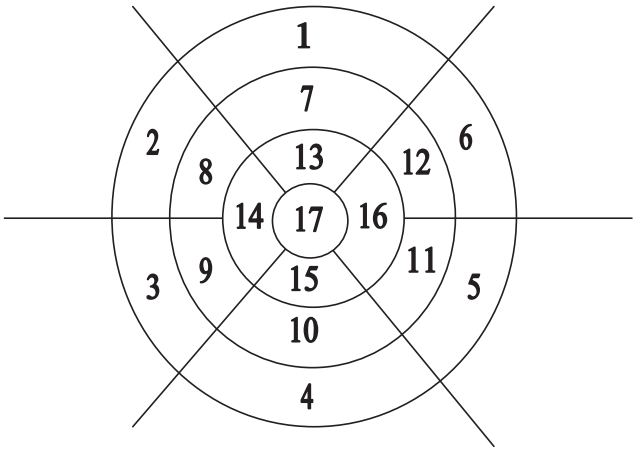

Fig. 1. Segmentation of the left ventricle at the short axis plane into 17 segment model in an anticlockwise manner. Basal level showed 6 segments (1, 2, 3, 4, 5 and 6), mid-cavitary level showed 6 segments (7, 8, 9, 10, 11 and 12), apical level showed 4 segments (13, 14, 15 and 16) and cardiac apex (segment 17).

Table 1
The correspondence of the ventricular segments to the culprit coronary territory. The LAD territory was the most affected (22 patients), RCA territory (10 patients) and LCX territory (8 patients).

	Coronary arterial territory					
	LAD (n=22)		RCA (n=10)		LCX (n=8)	
Segments	N	%	N	%	N	%
1	14	100.0	0	0.0	0	0.0
2	12	100.0	0	0.0	0	0.0
3	4	100.0	0	0.0	0	0.0
4	0	0.0	9	90.0	1	10.0
5	0	0.0	6	54.5	5	45.5
6	0	0.0	0	0.0	5	100.0
7	21	100.0	0	0.0	0	0.0
8	17	100.0	0	0.0	0	0.0
9	6	66.7	3	33.3	0	0.0
10	0	0.0	9	100.0	0	0.0
11	0	0.0	5	38.5	8	61.5
12	0	0.0	0	0.0	7	100.0
13	21	100.0	0	0.0	0	0.0
14	17	100.0	0	0.0	0	0.0
15	10	76.9	3	23.1	0	0.0
16	5	33.3	3	20.0	7	46.7
17	12	100.0	0	0.0	0	0.0

2.6. Data analysis

All cardiac MR images were analyzed to determine the presence or absence of myocardial enhancement (i.e. myocardial scarring) by 2 experienced observers. Myocardial scarring was considered if it involves more than 50% of the thickness for the diseased ventricular segment.

The culprit coronary artery was reported if LAD, RCA or LCX show occluded or significant stenotic lesion (reduction in the luminal diameter 70% or more) along the proximal or middle segments of their courses.

The left ventricle was divided into 17 segment model (Fig. 1) using the same landmarks of published study by Jose et al. based on short axis and long axis views [20]. Each myocardial scarred segment was analyzed and identified according to the correspondence culprit coronary artery, based on 17 segment model.

3. Results

Eighteen patients were excluded from the study, 11 patients with more than one significantly diseased

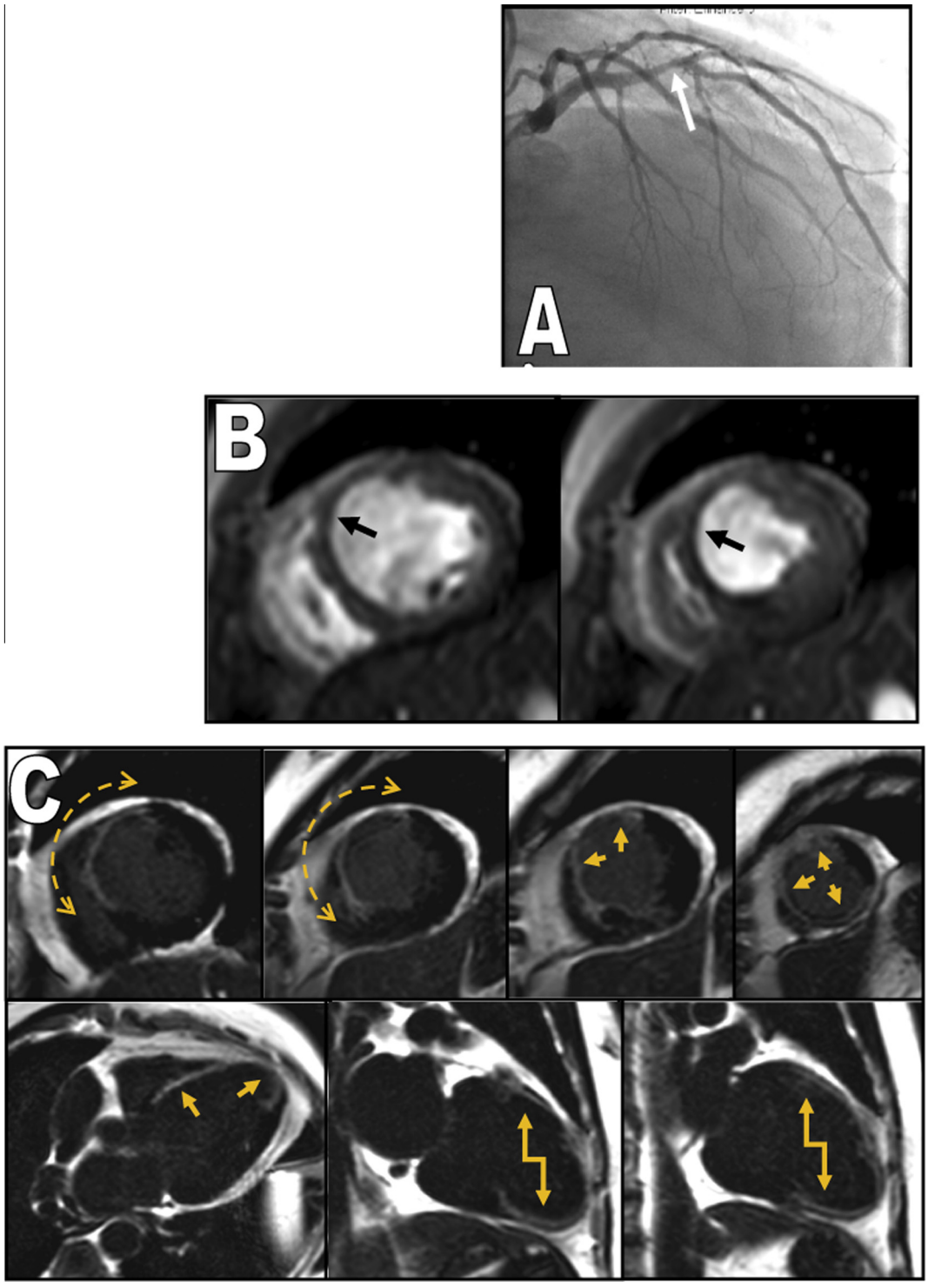

Fig. 2. (A) Coronary angiography showed significant stenosis of LAD. (B) Cine images during systole and diastole, showed marked thinning out and akinesia of the anterior, anteroseptal and septal wall of the left ventricle. (C) Post Gd DTPA IR sequence in short and long axis planes, showed enhancement and scarring along segments 1, 2, 3, 4, 5, 6, 13, 14 and 15.

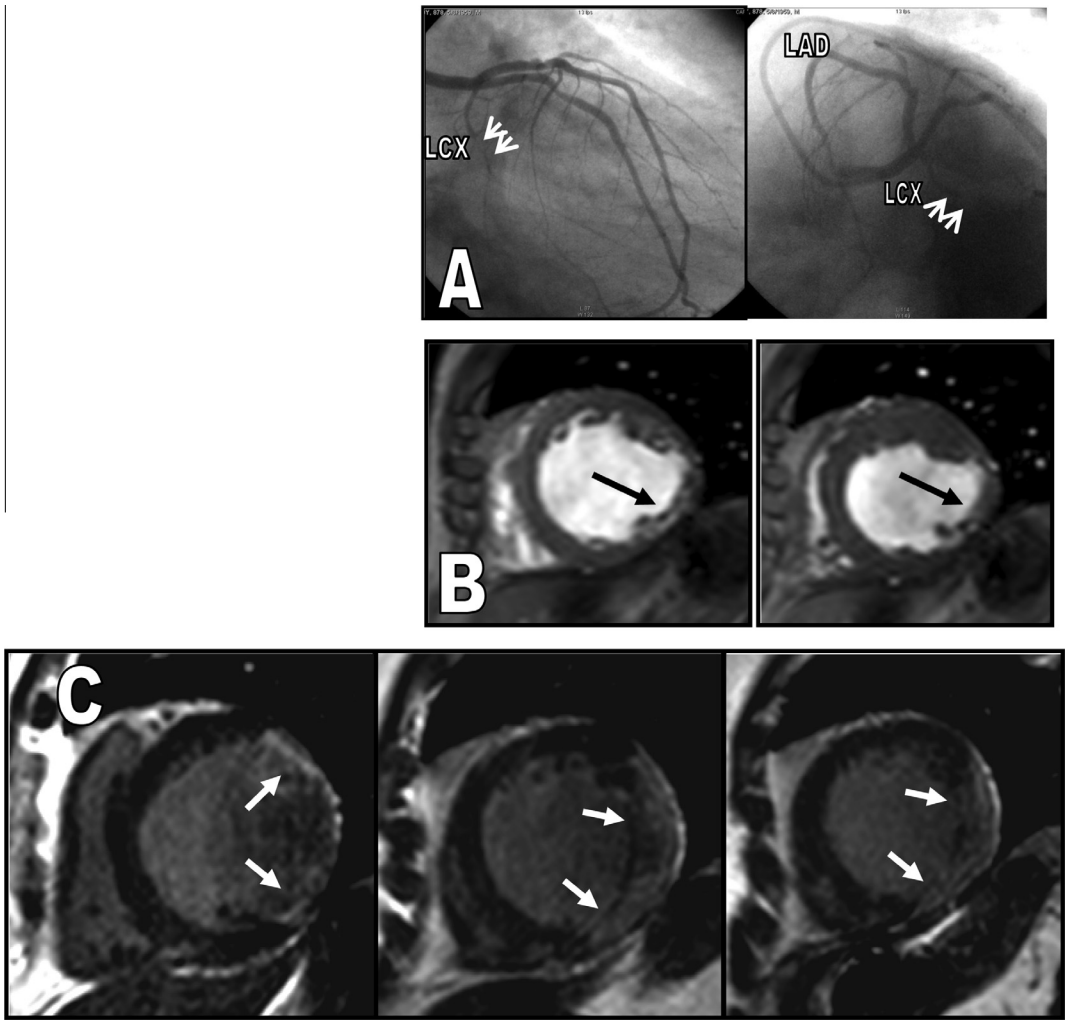

Fig. 3. (A) Coronary angiography showed totally occluded LCX after short proximal segment and then fills faintly antegradely. (B) Cine images during systole and diastole, showed marked thinning out and akinesia of the lateral and inferolateral wall of the left ventricle. (C) Post Gd DTPA IR sequence in short axis plane, showed enhancement and scarring along segments 11, 12 and 16.

coronary territory, 5 patients with no significant myocardial scarring and 2 patients couldn't complete the cardiac MR exam. And so, 40 patients were included in data analysis of this study.

The age of the patients ranged between 30 and 78 years old. There were a total number of 33 males and 25 females. All patients with myocardial scarring show variable degrees of motion abnormality (hypokinesia, akinesia and dyskinesia) and myocardial thinning out.

The LAD territory was the most affected in 22 patients, RCA territory in 10 patients and LCX territory in 8 patients (Table 1) and (Figs. 2–4). Based on per segment analysis, we found that 40 out of 210 (19%) segments with myocardial enhancement (ME) being mis-matched with the 17 segment model recommended by AHA.

We concluded that segments 1, 2, 3, 7, 8, 13, 14 and 17 were totally specific for LAD, and segments 6 and 12 were totally specific for LCX. Only segment 4 was totally specific for RCA and segment 10 was highly specific. There was overlap between LAD and RCA for segments 9 and 15 with slight LAD predominance. There was overlap between LCX and RCA for segments 5 and 11. Segment 16 was shared by the all territories (LAD, LCX and RCA) with slight LCX predominance (Figs. 5 and 6).

4. Discussion

The results were analyzed based on CMR per-segment analysis and compared to the 17-segment model recommended by AHA. Using this methodology and CMR imaging, we found that the coronary correspondence of 40 out of 210 segments (19.0%) with ME appears different from the 17-segment model in AHA. The disagreement was more evident at the basal antero-septal (segment 3), basal inferolateral (segment 5), apical inferior (segment 15) and apical lateral (segment 16) segments.

In our study, we found that 8 segments (segments 1, 2, 3, 7, 8, 13, 14 and 16) were totally specific for LAD and 2 segments (segments 6 and 12) for LCX and only one

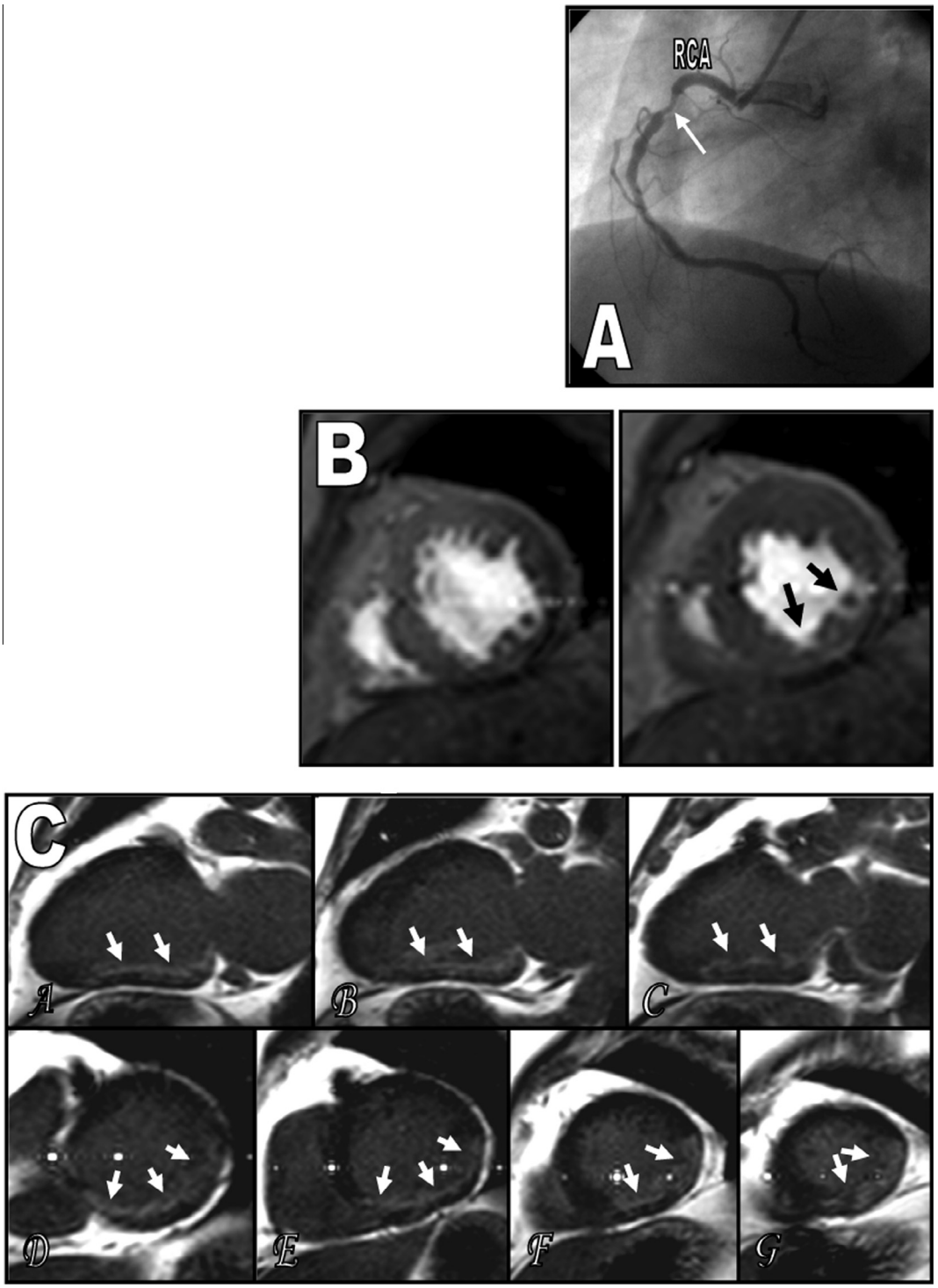

Fig. 4. (A) Coronary angiography showed significant stenosis of proximal RCA. (B) Cine images during systole and diastole, showed hypokinesia of the inferior and inferolateral wall of the left ventricle. (C) Post Gd DTPA IR sequence in short and long axis planes, showed enhancement and scarring along segments 4, 5, 10, 11, 15 and 16.

segment (segment 4) was totally specific for RCA (Figs. 5 and 6). Segment 10 was highly specific for RCA. The remaining 5 segments show much overlap between the different coronary arteries. These results almost explained by the individual variability of coronary artery distribution.

In contrast to the common belief that the apical inferior segment (segment 15) is supplied by the RCA as previously

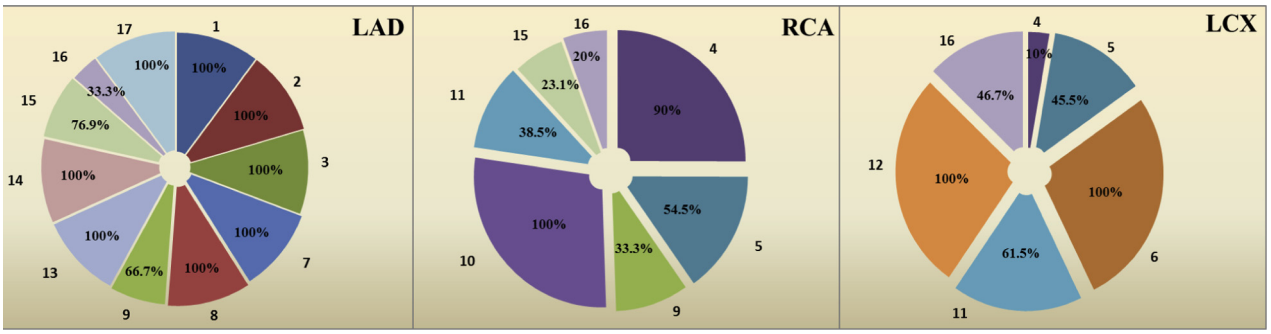

Fig. 5. Pie charts diagrams.

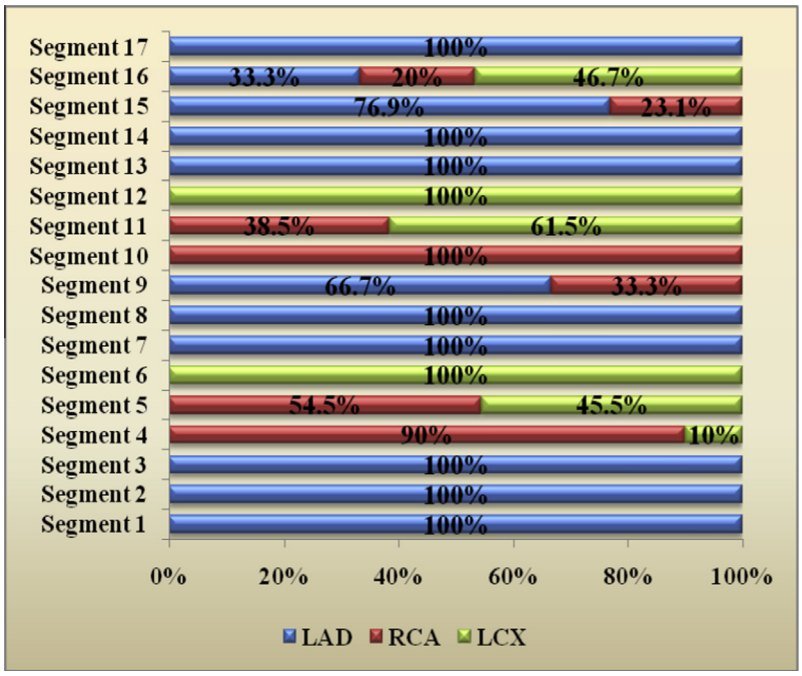

Fig. 6. According to the ventricular segmentation (17 segment model) and corresponding coronary artery territory.

recommended by AHA, our data suggested that it is highly specific to LAD (specific 77%) more than RCA territory (specific 23%) (Figs. 7 and 8).

Moreover, our study showed that the apical inferolateral segment (segment 16) not specific to one territory but shared and overlapped by the different three territories (Fig. 8) with slightly specific to LCX (47% specific for LCX, 33% specific for LAD and 20% specific for RCA).

The 17-segment model is widely used for the segmentation of the left ventricle [19]. Using different imaging modalities in analysis of coronary arteries to 17-segment model of the left ventricle resulted in wide range of variability.

Despite the high spatial resolution of CMR, only few previous studies are used for this analysis. From this point, our study aimed to analyze the correspondence of each scarred myocardial segment to the culprit coronary artery.

In a prospective study performed by Jose et al. [20] CMR was used to identify the ME of the left ventricle and conventional angiography to detect the corresponding culprit coronary artery. The per segment analysis used the 17-segment model. He found that 132 segments of ME out of 564 segments (23.4%) having different coronary distribution as compared to the 17-segment model in AHA. He found that only 4 segments (segments 2, 7, 8, and 13) totally specific for LAD occlusion as opposed to 8 segments in our study. However, we agree regarding the apical segments (segments 13, 14 and 15) were highly specific for LAD territory as well as that the different four apical segments (segments 13, 14, 15 and 16) could be affected in the LAD territory (Fig. 7).

Importantly, a previously reported study was performed by Pereztol-Valdés et al. [21] for patients with single culprit coronary artery disease. The study used nuclear

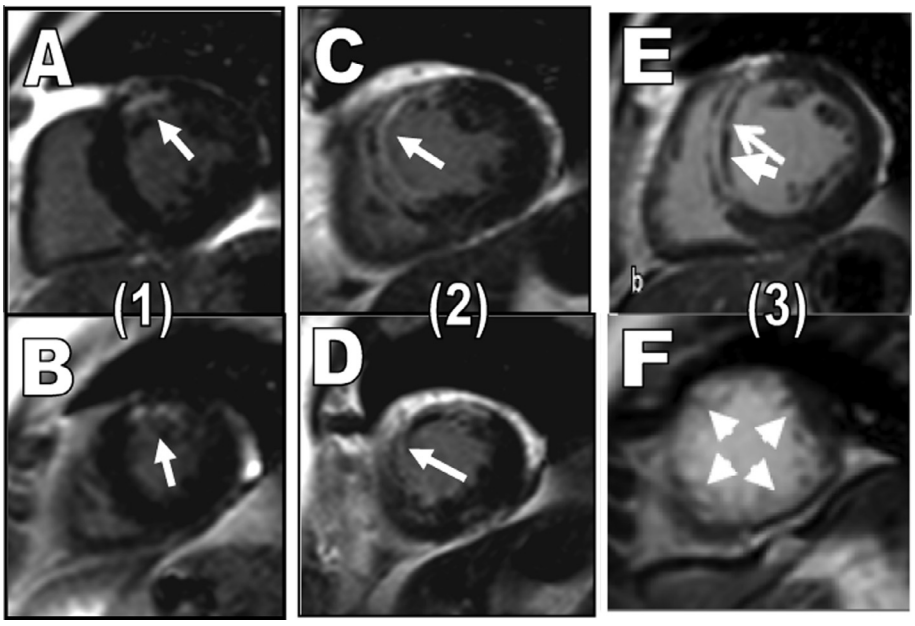

Fig. 7. Post Gd DTPA IR sequence in short axis planes, showed different enhancing segments for LAD territories in 3 different patients at the mid-cavitary and apical levels.

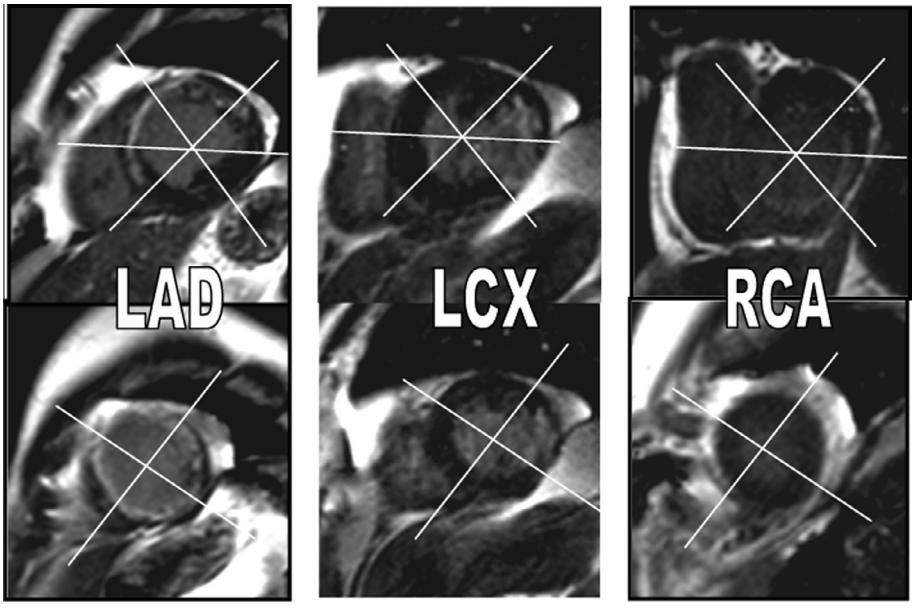

Fig. 8. Post Gd DTPA IR sequence in short axis planes at the mid-cavitary and apical levels in 3 different patients. Note the apical four segments can be affected in LAD territory. The inferior segment was not totally specific to RCA territory.

perfusion and percutaneous coronary intervention. In this study, 8 segments (segments 1, 2, 7, 8, 13, 14, 16, and 17) were found to be 100% specific for LAD occlusion. However, those 8 segments were different than in our study. This difference might be attributed to the difference in resolution between the CMR and the nuclear perfusion.

Many of the previous studies compared the sensitivity of SPECT myocardial perfusion against CMR as a modality of choice in detection of viability and perfusion defects [5,22]. Most of these studies revealed the higher sensitivity and specificity of CMR over SPECT.

In echocardiography the sub-endocardial fibrosis shows area of glistening reflecting the scarred area, while in ME-CMR, it is possible with high accuracy to detect the degree of involvement, and hence the viable underlying myocardium for revascularization.

Patients with chronic total coronary arterial occlusion are not necessary to have myocardial infarction and scar-

ring [23]. In such cases, coronary collateral circulations can explain the situations. Normal anastomosis between coronaries around the apex or at the crux is well known. However, in our study the explanation may also include that all patients had myocardial infarction which induced opening of the anastomosis as well as building up more and more collateral flow [24,25].

Recent studies of myocardial scarring and delayed enhancement in CT are being evolving, however not implicated in routine clinical practice when compared to CMR.

The current study discussed the CMR against other different modalities. Describing the coronary arterial tree using modalities of lower resolution caused great anatomical variability. Owing to the high resolution of CMR, our study is one of few studies in drawing the coronary territory using ME.

4.1. Study limitation

The limited number of included patients which didn't allow a wide range of variability regarding the coronary artery distribution because the CMR software package was not widely distributed.

5. Conclusion

Our study concluded that the distribution of LAD territory to the 17 segment model on CMR bases is larger than that proposed by AHA.

Conflict of interest

All authors have no conflict of interest.

References

[1] Lopez AD, Mathers CD, Ezzati M, Jamison DT, Murray CJ, editprs. Global burden of disease and risk factors: disease control priorities project. New York (NY): World Bank and Oxford University Press; 2006.

[2] Salerno Michael, Beller George A. Advances in cardiovascular imaging noninvasive assessment of myocardial perfusion. Circ Cardiovasc Imag 2009;2:412–24.

[3] Plein S, Ridgway JP, Jones TR, Bloomer TN, Sivananthan MU. Coronary artery disease: assessment with a comprehensive MR imaging protocol initial results. Radiology 2002;225:300–7.

[4] Misko J, Dziuk M, Skrobowska E, Szalus N, Pietrzykowski J, Warczynska A. Co-registration of cardiac MRI and rest gated SPECT in the assessment of myocardial perfusion, function and viability. J. Cardiovasc. Magn. Reson. 2006;8:389–97.

[5] Wagner A, Mahrholdt H, Holly TA, et al. Contrast-enhanced MRI and routine single photon emission computed tomography (SPECT) perfusion imaging for detection of subendocardial myocardial infarcts: an imaging study. Lancet 2003;361:374–9.

[6] Heller GV, Stowers SA, Hendel RC, Herman SD, Daher E, Ahlberg AW, et al. Clinical value of acute rest technetium-99 m tetrofosmin tomographic myocardial perfusion imaging in patients with acute chest pain and nondiagnostic electrocardiograms. J. Am. Coll. Cardiol. 1998;31:1011–7.

[7] Berman DS, Kiat H, Friedman JD, Wang FP, van Train K, Matzer L, et al. Separate acquisition rest thallium-201/stress technetium-99 m sestamibi dual-isotope myocardial perfusion single photon emission computed tomography: a clinical validation study. J. Am. Coll. Cardiol. 1993;22:1455–64.

[8] Hachamovitch R, Berman DS, Shaw LJ, Kiat H, Cohen I, Cabico JA, et al. Incremental prognostic value of myocardial perfusion single photon emission computed tomography for the prediction of cardiac death: differential stratification for risk of cardiac death and myocardial infarction. Circulation 1998;97:535–43.

[9] Taillefer R, DePuey EG, Udelson JE, Beller GA, Benjamin C, Gagnon A. Comparison between the end-diastolic images and the summed images of gated 99mTc-sestamibi SPECT perfusion study in detection of coronary artery disease in women. J Nucl Cardiol 1999;6:169–76.

[10] Vaduganathan P, He ZX, Vick GW, Mahmarian JJ, Verani MS. Evaluation of left ventricular wall motion, volumes, and ejection fraction by gated myocardial tomography with technetium 99 m-labeled tetrofosmin: a comparison with cine magnetic resonance imaging. J Nucl Cardiol 1999;6:3–10.

[11] Eisner RL, Martin SE, Leon AR, Schmarkey LS, Worthy MA, Chu TH, et al. Inhomogeneity of gated and ungated SPECT technetium-99 m-sestamibi bull's-eyes in normal dogs: comparison with thallium-201. J. Nucl. Med. 1993;34:281–7.

[12] Dilsizian V, Perrone-Filardi P, Cannon RO, Freedman NM, Bacharach SL, Bonow RO. Comparison of exercise radionuclide angiography with thallium SPECT imaging for detection of significant narrowing of the left circumflex coronary artery. Am. J. Cardiol. 1991;68:320–8.

[13] Kaul S, Senior R, Dittrich H, Raval U, Khattar R, Lahiri A. Detection of coronary artery disease with myocardial contrast echocardiography: comparison with 99mTc-sestamibi single photon emission computed tomography. Circulation 1997;96:785–92.

[14] Marwick T, D'Hondt AM, Baudhuin Twillemart B, Wijns W, Detry JM, Melin J. Optimal use of dobutamine stress for the detection and evaluation of coronary artery disease: combination with echocardiography or scintigraphy, or both? J. Am. Coll. Cardiol. 1993;22:159–67.

[15] Gregoire J, Theroux P. Detection and assessment of unstable angina using myocardial perfusion imaging: comparison between technetium-99 m sestamibi SPECT and 12-lead electrocardiogram. Am. J. Cardiol. 1990;66:42E–6E.

[16] Danias PG, Ahlberg AW, Clark BA, Messineo F, Levine MG, McGill CC, et al. Combined assessment of myocardial perfusion and left ventricular function with exercise technetium-99 m sestamibi gated single-photon emission computed tomography can differentiate between ischemic and non ischemic dilated cardiomyopathy. Am. J. Cardiol. 1998;82:1253–8.

[17] Kwok JM, Christian TF, Miller TD, Hodge DO, Gibbons RJ. Identification of severe coronary artery disease in patients with a single abnormal coronary territory on exercise thallium-201 imaging: the importance of clinical and exercise variables. J. Am. Coll. Cardiol. 2000;35:335–44.

[18] Brown KA, Heller GV, Landin RS, Shaw LJ, Beller GA, Pasquale MJ, et al. Early dipyridamole (99 m)Tc-sestamibi single photon emission computed tomographic imaging 2 to 4 days after acute myocardial infarction predicts in-hospital and postdischarge cardiac events: comparison with submaximal exercise imaging. Circulation 1999;100:2060–6.

[19] Cerqueira MD, Weissman NJ, Dilsizian V, Jacobs AK, Kaul S, Laskey WK, et al. Standardized myocardial segmentation and nomenclature for tomographic imaging of the heart. A statement for healthcare professionals from the cardiac imaging committee of the Council on Clinical Cardiology of the American Heart Association. Circulation 2002;105:539–42.

[20] Ortiz-Pérez JT, Rodríguez J, Meyers SN, Lee DC, Davidson C, Wu E. Correspondence between the 17-segment model and coronary arterial anatomy using contrast-enhanced cardiac magnetic resonance imaging. JACC: Cardiovasc Imag 2008;1:282–93.

[21] Pereztol-Valdés O, Candell-Riera J, Santana-Boado C, Angel J, Aguade-Bruix S, Castell-Conesa J, et al. Correspondence between left ventricular 17 myocardial segments and coronary arteries. Eur. Heart J. 2005;26:2637–43.

[22] Lee Vivian S, Resnick Daniel, Tiu Serafin S, Sanger Joseph J, Nazzaro Carol A, Israel Gary M, et al. MR imaging evaluation of myocardial viability in the setting of equivocal SPECT results with 99mTc sestamibi. Radiology 2004;230:191–7.

[23] Fefer P, Knudtson ML, Cheema AN, Galbraith PD, Osherov AB, Yalonetsky S, et al. Current perspectives on coronary chronic total occlusions: the Canadian multicenter chronic total occlusions registry. J. Am. Coll. Cardiol. 2012;59:991–7.

[24] Fulton WFM. Arterial anastomoses in the coronary circulation. I. Anatomical features in normal and diseased hearts demonstrated by stereoarteriography. Scottish Med J 1963;8:420–34.

[25] Conway EM, Collen D, Carmeliet P. Molecular mechanisms of blood vessel growth. Cardiovasc. Res. 2001;49:507–21.